Journal of Power Sources 188 (2009) 89–95

Contents lists available at ScienceDirect

Journal of Power Sources

journal homepage: www.elsevier.com/locate/jpowsour

Deactivation of Pt/VC proton exchange membrane fuel cell cathodes by SO2, H2S and COS

Benjamin D. Gould*, Olga A. Baturina, Karen E. Swider-Lyons

Code 6113, US Naval Research Laboratory, Washington, DC 20375, USA

ARTICLE INFO

Article history:
Received 29 September 2008
Received in revised form
12 November 2008
Accepted 14 November 2008
Available online 27 November 2008

Keywords:
Fuel cells
Hydrogen sulfide
Sulfur dioxide
Air contaminant
Platinum

ABSTRACT

Sulfur contaminants in air pose a threat to the successful operation of proton exchange membrane fuel cells (PEMFCs) via poisoning of the Pt-based cathodes. The deactivation behavior of commercial Pt on Vulcan carbon (Pt/VC) membrane electrode assemblies (MEAs) is determined when exposed to 1 ppm (dry) of SO_2, H_2S, or COS in air for 3, 12, and 24 h while held at a constant potential of 0.6 V. All the three sulfur compounds cause the same deactivation behavior in the fuel cell cathodes, and the polarization curves of the poisoned MEAs have the same decrease in performance. Sulfur coverages after multiple exposure times (3, 12, and 24 h) are determined by cyclic voltammetry (CV). As the exposure time to sulfur contaminants increases from 12 to 24 h, the sulfur coverage of the platinum saturates at 0.45. The sulfur is removed from the cathodes and their activity is partially restored both by cyclic voltammetry, as shown by others, and by successive polarization curves. Complete recovery of fuel cell performance is not achieved with either technique, suggesting that sulfur species permanently affect the surface of the catalyst.

1. Introduction

Successful operation of proton exchange membrane fuel cells (PEMFCs) requires that the membrane electrode assemblies (MEAs) maintain high activity for extended periods of time and avoid deactivation even under demanding environments. One deactivation mechanism is caused by the effects of common airborne contaminants on high surface area platinum electrocatalysts at the cathode. The cathode is particularly vulnerable in PEMFCs, as its oxygen reduction reaction (ORR) is the largest source of overpotential, or losses, in the MEAs. A recent review of PEMFC contamination studies emphasizes the need for further understanding of the fundamental mechanisms involved in cathode deactivation [1]. Understanding how common airborne contaminants deactivate the platinum electrocatalysts can help with design of sensible air purification systems and fuel cell operating specifications, and can also be used to develop operational strategies that prevent and recover fuel cells from deactivation, making low temperature fuel cells a more robust technology.

Sulfur compounds, such as SO_2, significantly degrade the performance of Pt electrocatalysts in fuel cell MEAs. Sulfur compounds deactivate heterogeneous catalysts by adsorbing to metal active sites, forming a strong chemical bond between sulfur atoms and the active metal catalysts [2,3]. MEA studies with sulfur-contaminated air indicate that both SO_2 and H_2S chemisorb to the Pt catalyst surfaces, disrupting the ORR and leading to decreased fuel cell current densities at constant cell voltage [4–10]. The previous MEA work was conducted over a wide range of contaminant concentrations (1–200 ppm H_2S) and varying exposure times (3–10 h). Nagahara et al. were the first to study the influence of sulfur species on MEA deactivation and reported similar voltage decay rates for MEAs exposed to SO_2 and H_2S when measured at a constant current density [11]. Another common air contaminant, carbonyl sulfide (COS), has not been studied in conjunction with SO_2 or H_2S.

This work endeavors to understand how different sulfur species influence the rate of fuel cell deactivation and how the loss of current density relates to sulfur coverage. Our approach is to compare the adverse effects of three adsorbed sulfur species, SO_2, H_2S, and COS, on MEA cathodes at multiple exposures times (3, 12, and 24 h), one cell voltage (0.6 V), and one concentration (1 ppm). This work expands upon the published literature on sulfur contamination by utilizing a combination of MEA deactivation experiments at constant voltage, polarization experiments and electrochemical characterization to ascertain the influence of speciation on deactivation and establish which airborne contaminants are the most deleterious in fuel cell operation; a distinction between our work and others' is that we measure the poisoning at a fixed voltage, which is more thermodynamically relevant, while others measure the poisoning at a fixed current density, [5,7,9,11], to predict how fuel cells might behave with a motor. With our approach, we strive to determine the behavior of individual sulfur species to help form

* Corresponding author. Tel.: +1 202 404 3359; fax: +1 202 404 8119.
E-mail address: benjamin.gould@nrl.navy.mil (B.D. Gould).

0378-7753/$ – see front matter © 2008 Elsevier B.V. All rights reserved.
doi:10.1016/j.jpowsour.2008.11.072

a basis for understanding the behavior of more realistic scenarios, i.e., air containing multiple contaminants.

Our testing procedure was based on a combination of methods from multiple sources. The fuel cell operating conditions and polarization measurement process were based on the method published by General Motors Fuel Cell Activities (GMFCA) [12]. The sulfur poisoning procedure and apparatus were based on the work by Mohtadi et al. and Moore et al. [5,7]. Cyclic voltammetry (CV) methods were based on the GMFCA method; our modified procedure included a slightly higher temperature (30 °C) and maximum sweep voltage (1.4 V) and our own cathode and anode flow rates [12,13]. During the testing sequence of each MEA, the H_2-crossover, polarization curves, and electrochemical surface area (ECSA) of the Pt cathode were monitored before and after contamination. The poisoning strength of the individual sulfur species was determined by measuring the loss of current density during the exposure of the MEA to SO_2, H_2S, and COS. After poisoning, the sulfur coverage, θ_S, of the Pt catalysts and changes in the catalysts' polarization behavior were measured for the three sulfur species.

Sulfur can be removed from the cathode catalyst via electrochemical cycling and exposure to neat air. Sulfur species adsorbed on the Pt can be electrochemically oxidized to water-soluble sulfate by a six-electron process with water at potentials greater than about 0.8 V vs. a reversible hydrogen electrode, by the reaction in Eq. (1) [14–16]:

$$Pt\text{–}S^0 + 4H_2O \rightarrow {SO_4}^{2-} + 8H^+ + 6e^- + Pt \quad (1)$$

The resulting sulfate desorbs from the electrocatalyst surface, allowing recovery of the catalyst performance. Sulfur also can be oxidized to sulfate by a redox process with platinum oxide (or platinum hydroxide) and water [17,18].

The findings of this work are discussed in the context of probable deactivation mechanisms, sulfur coverage, and mass transfer limitations involved during fuel cell operation. The relevance of airborne contaminants to fuel cell operation will be emphasized and possible recovery strategies for deactivated fuel cells will be proposed.

2. Experimental

Commercially available catalyst-coated membranes (CCMs) from Ion Power, Inc. were used to make the MEAs. The CCMs consisted of two 10 cm^2 square layers of catalyst ink deposited on opposite sides of a 50-μm thick NRE 212 Nafion membrane. Both the anode and cathode catalysts were 50 wt.% Pt supported on Vulcan carbon, which equates to a Pt loading of 0.4 $mg_{Pt}\,cm^{-2}$ (geometric). A single cell was constructed by placing one CCM between two gas diffusion layers (SGL 25 BC, 256 μm), an anode side 200 μm Teflon gasket (electronics grade) and a cathode side 150 μm Teflon-coated fiber glass gasket inside a test fixture from Fuel Cell Technologies. Cartridge heated end plates, current collectors, Poco graphite flow fields with single serpentine flow channels, gaskets, GDLs, and the MEA were all sealed together with eight bolts at 10 N m of torque per bolt.

Once assembled, the performance of the single cell MEA was tested using an 850e Fuel Cell Test System from Scribner Associates, Inc. All experiments were conducted at 80 °C and 100% RH, unless otherwise noted. Humidifiers were filled with 18 MΩ cm water from a Barnstead Nanopure system. The anode gas was ultra-high purity H_2 (99.999% Praxair). The cathode air feed was ultra-zero air (99.999% N_2/O_2 Praxair), except during the poisoning experiments described below. The H_2 flow was always 0.25 SLPM, except during polarization curves when an air/fuel stoichiometric ratio was 2/2, with the absolute flow dependent on the load. New MEAs were used for each experimental condition and each experiment was repeated at least twice.

All experiments started by breaking in the membrane by alternating the cell between 0.7 V for 1 min and 0.5 V for 9 min over a 12-h period during which the current density of the cell became constant. After breaking-in, the cell was cooled to 30 °C under a flow of 0.03 SLPM Ar to the cathode. Both humidifiers were cooled to 50 °C. Once the cell was cooled and the open circuit potential (OCP, approx. = 0.1 V with respect to RHE) had reached steady state, CV was performed from OCP to 1.4 V to OCP on the MEAs using an Autolab™ PSTAT30 potentiostat to clean the Pt surface. All CV measurements were performed using the anode under flowing H_2 as the reference electrode.

The current density of each MEA before poisoning was determined by heating the cell back up to 80 °C and holding its voltage constant for 8–12 h. Next, the polarization curves of un-poisoned MEAs were measured from 0.5 to 0.9 V. The current interrupt method was used to determine and correct for the cell's resistance during polarization experiments. After the polarization curves of un-poisoned MEAs were measured, the cathode was flushed again with Ar and the H_2-crossover was measured at 80 °C. Then, the cell was cooled to 30 °C under Ar and the ECSA of the un-poisoned MEAs were determined using CV at 50 mV s^{-1}. The ECSA was determined from the charge consumed during hydrogen desorption between the OCP and 0.4 V, after double layer correction, assuming 210 μC cm^{-2} as a conversion factor [12].

With characterization of the un-poisoned MEA complete, sulfur contamination experiments were commenced. The cell was heated back to 80 °C and held at 0.6 V for 2 h until the current density was stable with a cathode feed of 0.5 SLPM ultra-zero air. Once a baseline current density was established, sulfur species were introduced directly into the cathode air feed through a heated Teflon inlet downstream of the humidifiers. Certified mixtures of 5 ppm SO_2 in ultra-zero air, 5 ppm H_2S in ultra-zero air, and 5 ppm COS in ultra-zero air (Praxair) were used as the starting compositions for the contamination studies. The 5 ppm contaminant feeds were mixed with humidified incoming cathode air and diluted to 1 ppm of each sulfur species on a dry-gas basis. Gas dilution was accomplished by two MKS mass flow controllers and the total gaseous flow rate into the cathode was maintained at 0.5 SLPM (dry). The cell was held at 0.6 V. The humidity of the pure cathode air was adjusted so that, when mixed with the dry contaminant gas, the humidity entering the cell would remain at 100% RH. The deactivation procedure with 1 ppm of all three sulfur species was performed at three different exposure times: 3, 12, and 24 h.

At the completion of the sulfur poisoning experiments, the poisoned MEA was characterized. The cell was held at 0.6 V while the cathode was flushed with ultra-zero air for 8–10 h to remove any traces of unreacted sulfur species in the experimental apparatus. The ultra-zero air was replaced with Ar at the above flow rates and the H_2-crossover was measured at 80 °C. Then, the cell was cooled to 30 °C and CV was performed on the cathode to determine sulfur coverage, θ_S, from the difference in charge over the hydrogen desorption region of the CV [14], as written in Eq. (2)

$$\theta_S = \frac{Q_{10} - Q_1}{Q_{10}} \quad (2)$$

In this equation, Q_1 and Q_{10} are the charges from the hydrogen desorption regions of the contaminated surface and of the clean surface, respectively. Use of the equation assumes that one sulfur atom adsorbs to one platinum atom and that the sulfur does not significantly deactivate any adjacent platinum sites for hydrogen adsorption.

There is disagreement in the literature on the correct adsorption stoichiometry for S on Pt because it is common for a single sulfur atom to poison multiple adjacent Pt sites [2,14,19–21]. The reported adsorption stoichiometries range from 1 to 12 Pt atoms per S atom. Our method of calculating sulfur coverage represents

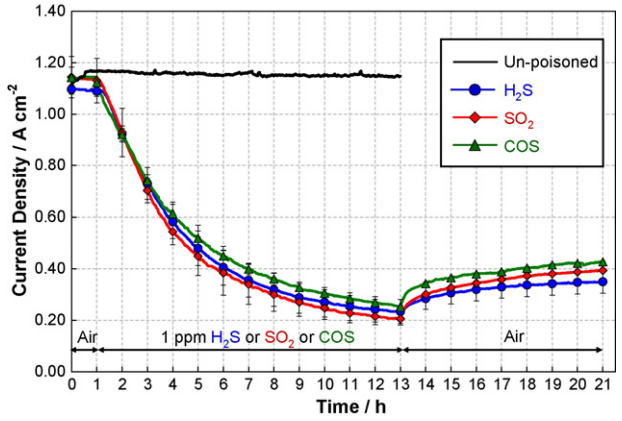

Fig. 1. Current density loss during exposure of platinum on Vulcan carbon (Pt/VC) to 1 ppm H_2S for 12 h, 1 ppm SO_2 for 12 h, 1 ppm COS for 12 h at E_{cell} = 0.6 V. Followed by recovery in air for 8 h at E_{Cell} = 0.6 V.

an upper bound for the amount of sulfur present on the surface of Pt. If a different adsorption stoichiometry was proven to be definitive, it would alter only the absolute magnitude of our sulfur coverages, θ_S, but not the trends in exposure time. It would be a trivial matter to recalculate new sulfur coverages, θ_S. This has been the approach suggested by Langer and co-workers [20].

Sulfur coverage determined from the hydrogen desorption region is a measure of how many hydrogen desorption sites have been blocked by sulfur $(1-\theta_H)$, making this method an indirect measure of the sulfur coverage. We could not measure sulfur coverage directly through integration of the sulfur oxidation region because of difficulty deconvoluting current contributions from oxidation of sulfur, oxidation of Pt, and oxidation of the carbon support.

After the sulfur coverage was determined, the cell was heated to 80 °C and a second set of polarization curves were measured to determine the percentage of performance recovered by CV. After the polarization curves, a second exposure to sulfur species was performed, followed by flushing with ultra-zero air. After flushing with air, a third set of polarization curves were measured from 0.5 to 0.9 V with sulfur on the surface under the same load based flow used for the determination of un-poisoned behavior.

3. Results

The current density vs. time of the Pt/VC-based MEAs is shown in Fig. 1 during the exposure of their cathodes to air contaminated with 1 ppm of SO_2, H_2S, or COS over a 12-h period followed by the recovery in neat air for 8 h, while the cell is held at 0.6 V. The data for each sulfur species are the average of three separate deactivation experiments with error bars corresponding the standard deviation of the data set. All three of the sulfur impurities, SO_2, H_2S, and COS, cause the same loss of current density vs. time within experimental error. All MEAs undergo a rapid loss of activity in the first 3 h of exposure to the sulfur contaminants, followed by an asymptotic approach to a saturation current density, presumably due to the equilibration of the Pt electrocatalysts with the contaminants. The saturation current density is approximately 0.22 A cm^{-2} for all three sulfur-contaminated MEAs. The current density improves slightly after the MEA is operated for 8 h with neat air at 0.6 V and probably due to the removal of weakly adsorbed sulfur species by reaction with oxygen [20]. Our results are analogous to the similar voltage decay rates observed when MEAs are exposed to SO_2 and H_2S at constant current density [11].

The sulfur coverage of the S-contaminated Pt nanoparticles can be elucidated from cyclic voltammetry measurements. Fig. 2 shows the first voltammetric cycle from 0.09 to 1.4 V to 0.09 V measured under Ar for the Pt/VC cathodes after exposure to the SO_2, H_2S, or COS contaminants in air. Each voltammogram shows the same characteristic sulfur oxidation features on Pt/VC, independent of poisoning species identity, with a sharp sulfur oxidation peak at 0.8 V (I) and two broad peaks at 1.05 and 1.15 V (II and III). The identical nature of the CVs does not necessarily offer information about the *in situ* structure of adsorbed sulfur compounds on the cathode during contamination, as the electrode acquires a potential of 0.1 V as it cools under an inert gas prior to cyclic voltammetry. During the cooling process when the potential decreases to 0.1 V, the sulfur compounds formed *in situ* on the Pt surface from individual contaminants are presumably all reduced to adsorbed S^0, if all of the individual contaminants are not initially adsorbed as S^0.

Our CV results are similar to the work of Contractor and Lal, who showed that the voltammograms of adsorbed SO_2 and H_2S in solution on a Pt-wire were identical when the electrode is taken to 0 V [22]. At 80 °C, it has been shown that two features exist in the oxygen adsorption region of the voltammograms; it has been postulated that these features represent a linear and bridged form of sulfur on the Pt surface, signifying both a weakly and strongly bonded sulfur species [16,22,23]. These two sulfur oxidation peaks occur at 0.97 and 1.10 V. Three oxidation peaks were observed in our work (I–III). The two peaks in our work at 1.05 and 1.15 V could correspond to oxidation of the two sulfur species postulated by Contractor and Lal. The slight difference in our oxidation peak voltages is probably caused by our lack of a true reference electrode and differences in surface roughness of our working electrode. Our working electrode is a high surface area Pt catalyst dispersed on carbon and our reference electrode is the anode of the MEA, while the working electrode of Contractor and Lal was a low surface area piece of platinized wire with a reversible hydrogen electrode as the reference electrode. Additionally, our oxidation features include contributions from the oxidation of the carbon support and the oxygen evolution reaction.

Four successive voltammograms are shown in Fig. 3 for a cathode after exposure to 1 ppm H_2S for 24 h at 0.6 V. The first potential sweep in green (CV 1) is dramatically different when compared to the other three voltammograms. This voltammogram shows much lower features in the hydrogen desorption region (0.08–0.3 V) and much higher features in the sulfur oxidation region (0.7–1.4 V) than the following voltammograms. There is also a slight depression in the oxidation region of the voltammogram from 0.8 to 0.93 V. Ten scans are taken for each experiment. After four successive scans,

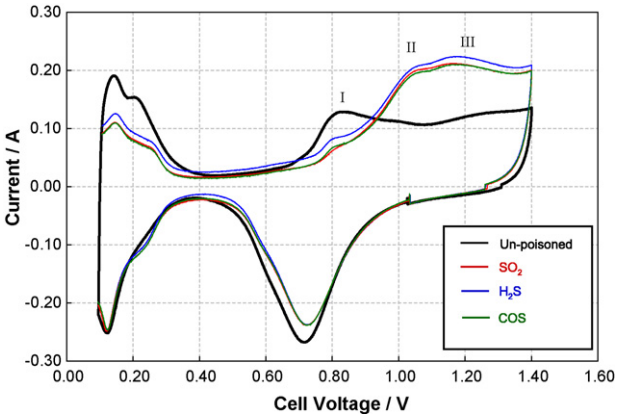

Fig. 2. The initial cyclic voltammogram of Pt/VC after exposure to 1 ppm H_2S (blue), 1 ppm SO_2 (red), and 1 ppm COS (green) at 0.6 V for 24 h; polarization program OCP → 1.4 V → OCP at ν = 50 mV s^{-1}. H_2/Ar (anode/cathode), 30 °C-cell, and 50 °C-humidifiers. (For interpretation of the references to color in this figure legend, the reader is referred to the web version of the article.)

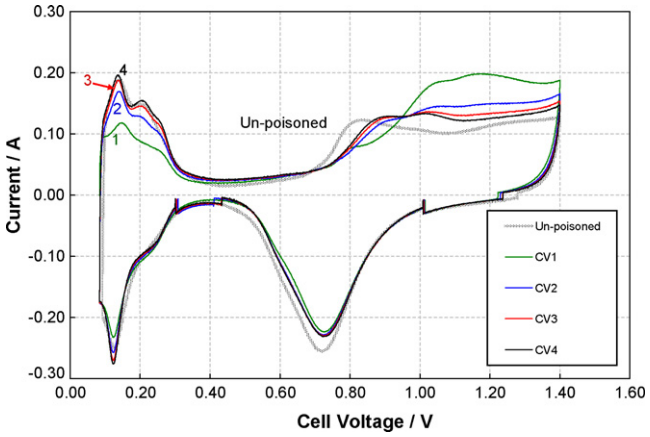

Fig. 3. Successive cyclic voltammograms of Pt/VC after exposure to 1 ppm H_2S at 0.6 V for 12 h; polarization program OCP → 1.4 V → OCP at $\nu = 50\,mV\,s^{-1}$. H_2/Ar (anode/cathode), 30 °C-cell, and 50 °C-humidifiers.

the CV becomes stable and returns to the shape observed for clean platinum in the hydrogen desorption region. Similar curves are observed after exposure to both 1 ppm SO_2 and 1 ppm COS for 12 h in a cell at 0.6 V.

Comparison of the fourth potential sweep (CV 4) and the un-poisoned MEA shows that the oxidation feature at 0.8 V is never fully recovered and a new oxidation feature exists at 1.03 V. The oxidation peak at 0.8 V is shifted to 0.9 V when the un-poisoned MEA is compared to fourth potential sweep (CV 4). This feature at 0.8 V is usually assigned to Pt oxidation of highly dispersed metal crystallites and suggests that the adsorbed sulfur has influenced this reaction [24,25]. The change in the CV may represent a reconstruction of the Pt surface or increase in the Pt particle size. Surface reconstruction has been observed experimentally during adsorption of SO_2 on Pt (1 1 1) in electrochemical conditions [26]. Surface reconstruction also is predicted to occur during the adsorption of SO_2 onto Pt (1 1 1) by density functional theory (DFT) [27]. Another possible explanation for the change in the CV is the re-adsorption of sulfate anions produced in Eq. (1) [21]. Our inability to completely recover the voltammogram of an un-poisoned MEA through cyclic voltammetry differs from the results seen in solution-based poisoning experiments, which show that complete recovery of the electrode is possible [28].

When the sulfur coverage is plotted vs. exposure time, the saturation of the sulfur coverage becomes evident. The first ordinate of Fig. 4 depicts the sulfur coverage at increasing exposure times of 0, 3, 12, and 24 h for 1 ppm of all three sulfur species adsorbed at 0.6 V

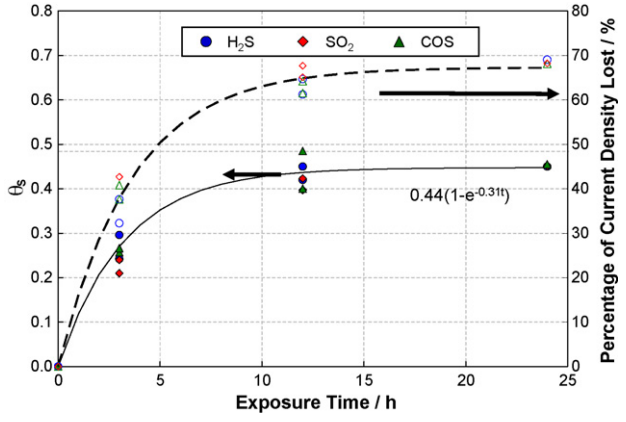

Fig. 4. Saturation of sulfur coverage (θ_s) (solid) for H_2S, SO_2, and COS at varied exposure times compared to the percentage of current density lost (dashed).

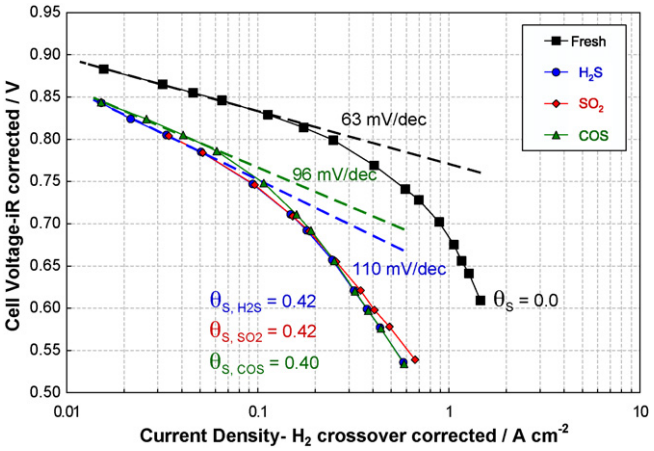

Fig. 5. Polarization curves in Tafel coordinates of MEAs after exposure to 1 ppm H_2S (blue), 1 ppm SO_2 (red), and 1 ppm COS (green) for 12 h and 0.6 V, showing the change in Tafel slope and loss of current density. (For interpretation of the references to color in this figure legend, the reader is referred to the web version of the article.)

and 80 °C. Sulfur coverage approaches an asymptote at 0.45 and changes by less than 1% when the exposure time was doubled from 12 to 24 h. The second ordinate of Fig. 4 shows the percentage of current density lost after each exposure time followed by recovery in air. When sulfur coverage and loss of current density are compared vs. exposure time, the trends are strongly correlated. This saturation of sulfur coverage mirrors the plateau of current density observed during deactivation. The plateau in current density during deactivation is caused by a saturation of the sulfur coverage. Note that exposure to 1 ppm H_2S for 12 h corresponds to approximately three theoretical monolayers (ML) if all of the sulfur atoms were adsorbed to the Pt surface, assuming an adsorption stoichiometry of one sulfur atom to one platinum atom and that the ECSA is the relevant surface area for adsorption.

Polarization curves are performed on the sulfur covered surface after the second exposure to sulfur species. Fig. 5 shows three typical polarization curves after the MEA is exposed to 1 ppm SO_2, H_2S, and COS for 12 h at 0.6 V, with one polarization curve of an un-poisoned MEA for comparison. The polarization curves show the expected trend of lower performance at higher sulfur coverages. The kinetic region of the polarization curve shows an increase in both the activation overpotential for ORR and the Tafel slope with sulfur on the surface. The Tafel slope increases from the typical $61 \pm 2.4\,mV\,dec^{-1}$ observed in the un-poisoned Pt/VC MEAs to approximately $92 \pm 11\,mV\,dec^{-1}$ at a sulfur coverage of 0.4 (measured by CV). The increased Tafel slope of poisoned Pt is difficult to interpret in this potential region (0.8–0.9 V) where adsorbed sulfur species are oxidized to sulfate in parallel with oxygen reduction.

After the MEAs are deactivated by sulfur, attempts are made to recover the performance of the cell by removing the sulfur from the surface. Two possible strategies of recovery are utilized during this work. One strategy is to employ CV to "clean" the surface by oxidizing the sulfur into sulfate electrochemically. The other method is to use successive polarization curves to clean the surface. The effectiveness of the two strategies is shown in Fig. 6. Cleaning the surface by CV is not a new idea and has been shown to be effective in the previous literature [28,29]. Our metric for cell recovery was the ratio of the power density at 0.6 V after the recovery procedure to the power density at 0.6 V of the un-poisoned cell. It is possible to recovery 92% of the power density through CV (green squares). Cell recovery by successive polarization curves after exposure to sulfur show a power density recovery of 85% (blue lines). It appears that by first exposing the MEA to a voltage of 0.9 V, and then lowering the voltage back to 0.5 V, it is possible to remove

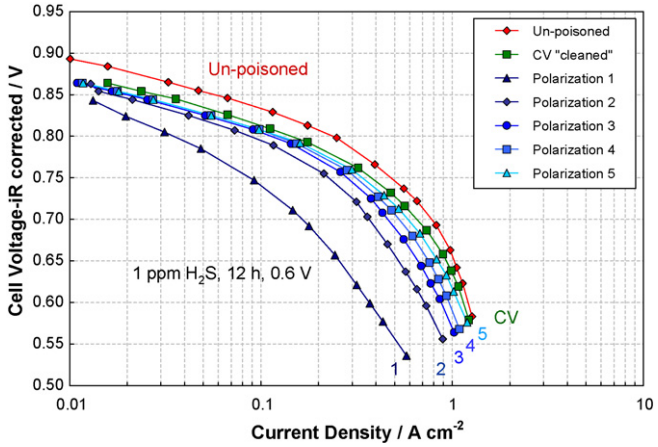

Fig. 6. Polarization curves in Tafel coordinates of a un-posioned Pt/VC MEA (red), after H_2S adsorption removed by cyclic voltammetry (CV) (green), and with sulfur on the surface (blue 1–5) with successive polarization curves showing cell current density recovery. (For interpretation of the references to color in this figure legend, the reader is referred to the web version of the article.)

sulfur from the surface. CV measurements confirm that the sulfur coverage is approximately 0.1 after five successive polarization curves.

4. Discussion

The results above indicate that Pt/VC cathodes exposed to 1 ppm of SO_2, H_2S or COS in air all show the same deactivation behavior. All of the cathodes saturate with a sulfur coverage of around 0.45, or when 45% of the surface Pt atoms have adsorbed sulfur.

The loss of current density vs. time depicted in Fig. 1 represents transient current response caused by a given concentration of sulfur species. The deactivation of the catalytic surface of the cathode should relate to how many sites are being deactivated by adsorbed sulfur species. To interpret these results, we consider the mechanisms by which sulfur species might deactivate the Pt electrocatalysts in the working fuel cell cathodes.

SO_2 adsorption from the gas phase onto Pt has been studied extensively. Single crystal studies, supported catalyst studies, and density functional theory all suggest that sulfur chemisorbs as a SO_x species [27,30–32]:

$$Pt + SO_2 \rightarrow Pt\text{–}SO_x \quad (3)$$

The sulfur coverage affects the value for x in the SO_x (0–4) and the coordination of the surface bound moiety with the Pt surface, according to DFT [27,31,32].

The adsorption of SO_2 in solution onto Pt electrodes has been investigated comprehensively; the final oxidation state of sulfur strongly depends on the electrode potential in the electrochemical cell [14,16,21–23,28,33–38]. At low potentials (0.05–0.4 V), adsorbed sulfur species on platinum are converted to zero-valent sulfur. At high potentials (0.8–1.4 V), zero-valent sulfur and adsorbed sulfur species on platinum are oxidized to sulfate (SO_4^{2-}) in acid electrolyte, as demonstrated spectroscopically [39,40]. At intermediate potentials (0.4–0.8 V), the oxidation state and the chemical identity of the adsorbed sulfur species from SO_2 on Pt electrodes remains open to debate, although many researchers believe that adsorbed sulfur species exist as zero-valent sulfur [14,16,20]. This view has been challenged by others who believe that sulfur exists as a platinum sulfide (−2 valence state) [21,33,41]. The existence of sulfur bilayers at high sulfur coverages also has been proposed [16,22,23].

Cathode deactivation by H_2S is believed to follow the reaction in Eq. (4), which is adopted from studies of gas phase adsorption of H_2S onto a Pt/Al_2O_3 catalyst in vacuum [5,38]:

$$H_2S\text{–}Pt \rightarrow Pt\text{–}S + H_2 \quad (4)$$

Solution-based electrochemistry supports the formation of $Pt\text{–}S^x$ in the presence of H_2S, but the oxidation state of the sulfur in $Pt\text{–}S^x$ still remains in question [14,22,33].

Information on the interaction between COS and Pt surfaces is very limited. Spectroscopic evidence suggests that COS chemisorbs both dissociatively and non-dissociatively on Pt/Al_2O_3 by the mechanisms in Eqs. (5) and (6) [42]:

$$Pt + COS \rightarrow Pt\text{–}COS \quad (5)$$

$$Pt\text{–}COS + Pt \rightarrow Pt\text{–}CO + Pt\text{–}S \quad (6)$$

The literature suggests that the exposure of Pt nanoparticles to SO_2, H_2S and COS would lead to a range of products, including $Pt\text{–}SO_x$, Pt–S, and Pt–CO. Furthermore, the severity of a sulfur poison is generally ranked by sulfur's oxidation state, making the order of toxicity: $H_2S > COS > SO_2$ [3]. Our results show the identical electrochemical behavior, independent of the original sulfur species.

There are three plausible explanations for the observed similarity in the deactivation behavior of the three sulfur compounds in Fig. 1. The first explanation is that both H_2S and COS are converted homogeneously to SO_2 before they ever reach the fuel cell; thus, all sulfur deactivation is actually SO_2 deactivation. This is plausible because both H_2S and COS are flammable gases capable of combustion in humid air by the following reactions [43,44]:

$$2H_2S + 3O_2 \rightarrow 2SO_2 + 2H_2O \quad (7)$$

$$2COS + 3O_2 \rightarrow 2SO_2 + 2CO_2 \quad (8)$$

A second possible explanation is that all three sulfur species follow reaction paths to the same rate determining step when they adsorb on platinum. Numerous possible rate determining steps satisfy this condition. One hypothetical rate determining step could be the catalytic combustion of sulfur species to a SO_x surface species or, the rate determining step could be the desorption of adsorbed oxygen to free a site for sulfur adsorption.

A third possible explanation for the similarity in deactivation behavior is that the observed transient current response (current loss vs. time) is limited by the rate of mass transfer of the sulfur species at low concentrations to the catalyst surface at these temperatures and voltages. Essentially, the rate of diffusion of the contaminant species from the gas stream in the flow channel through the gas diffusion layer, into the catalyst pore structure, through the ionomer, and onto the Pt surface is much slower than the rate of SO_2, H_2S, and COS adsorption (reactions (3), (4), and (5)). This would cause the observed rate of deactivation to be related to mass transfer and not catalytic deactivation. Assuming the effective diffusivity from the flow channel to the catalyst surface is the same for all three sulfur species, this would cause the transient current response to be equivalent. All three species could approach the same saturation current density if the final adsorbed poisoning species were the same between the individual sulfur species. This would explain the observed independence of deactivation behavior from the sulfur species identity.

One argument against a mechanism governed by mass transfer limitations is that the gas phase diffusion coefficients depend on species identity and are different for SO_2, H_2S and COS. The binary diffusion coefficients of the sulfur species in air at 80 °C can be estimated from the kinetic theory of gas. Using the Wilke–Lee modification of the Hirschfelder–Bird–Spotz method, the binary diffusion coefficients for SO_2, H_2S, and COS are estimated to be

1.9×10^{-5}, 2.5×10^{-5}, and 1.9×10^{-5} $m^2\ s^{-1}$, respectively [45]. The SO_2 and COS diffusion coefficients are identical, while the diffusion coefficient of H_2S is 30% greater than those of SO_2 and COS. A difference of 30% is well within the accuracy of this comparison, given binary diffusion coefficients are an over simplification of the actual sulfur species diffusion in the fuel cell. The tortuous path of the adsorbate to the surface in a fuel cell may nullify any differences between the three species. Additionally, there is some support for this hypothesis in the aqueous poisoning literature, which suggests that H_2S poisoning at certain conditions can be diffusion controlled [37].

The saturation behaviors observed in Figs. 1 and 4 are typical for many catalytic systems experiencing deactivation; this effect can be rationalized as the catalytic surface reaching its adsorption capacity of the poisoning species [46]. Our sulfur coverage vs. exposure time data in Fig. 4 can be fitted accurately with a simple exponential function similar to the function used by Mohtadi et al. [6]. A quantitative comparison between our work and the experiments in the literature is difficult because different operating parameters are used in each work; moreover, the decreases in cell voltage during sulfur exposure are often monitored at constant current instead of current loss at constant cell voltage [1,47]. Qualitatively, sulfur deactivation data in the literature show the same trends as our work; during deactivation, some form of saturation behavior exists with exposure time on both the anode and the cathode of fuel cells [5,6,10,47]. The saturation behavior is most pronounced at lower concentrations (~1 ppm H_2S/H_2) and lower current densities (100–500 mA cm^{-2}) [1].

The similarities between our work and previous literature depart when the magnitude of the sulfur coverage is compared. We observe that sulfur coverage approaches saturation around 0.45, while the literature reports sulfur coverages approaching 1.0 [6,16,19,20,22,36,48]. The sulfur coverage calculated by Mohtadi et al., was the ratio of the sulfur oxidation charge for a specific exposure time divided by maximum sulfur oxidation charge reached at infinite time [6]. This definition of sulfur coverage forces the values to range from zero to unity; it represents the percentage of saturation, but not the actual number of Pt atoms blocked by sulfur on the surface. The sulfur coverage measured on Pt electrodes in solution was calculated using the charge from both the sulfur oxidation and hydrogen desorption regions of the CV [16,19,20,22,36].

The differences between the sulfur coverage observed in our work and the sulfur coverages reported in the preceding literature can be explained by differences in the reaction environments when the sulfur was adsorbed. Sulfur adsorption in our experiments occurs in the presence of gaseous oxygen and sulfur coverage is measured after the MEA is partially recovered by an air purge. In other work, sulfur adsorption on Pt electrodes takes place in a deoxygenated electrolyte, which is much different than operating fuel cell cathode [16,19,20,22,36]. The saturation behavior observed in our work likely is caused by competitive adsorption between oxygen and sulfur. Deactivation models for anode poisoning predict that saturation is caused by competitive site adsorption between hydrogen and sulfur [47]. The resistance of platinum oxide to sulfur poisoning has been shown in earlier work [17,18]. The influence of adsorption of SO_2 onto oxygen covered Pt surfaces has been studied by DFT [27]. The DFT suggests that the sulfur adsorbs as SO_x species on the surface, with SO_4^{2-} being the most stable form of oxidized sulfur. Electrochemical experiments in solution have shown that the presence of oxygen in solution can decrease the sulfur coverage from 1.0 to 0.2 [20].

Fig. 6 shows that recovery is possible by cycling the cell up to 0.9 V. This may be additional evidence of the competitive adsorption between oxygen and sulfur with Pt–O species likely to be formed at voltages close to open circuit voltage (OCV). It has been observed that sulfur poisoned anodes show improved recovery when the cell is exposed to OCV, but it is unclear how changing the voltage at the cathode influences the chemistry of the anode [9]. It appears that increasing the cell voltage to 0.9 V is an effective way of removing sulfur from the surface, by entering the region of electrochemical sulfur oxidation observed during cyclic voltammetry. All this evidence suggests that the presence of oxygen on the surface or in the gas phase plays an important role in determining the behavior of fuel cell deactivation by gas phase sulfur species.

5. Conclusions

We examined the deactivation behavior of commercial Pt/VC MEA catalysts when the cathode was exposed to three different sulfur species: SO_2, H_2S, and COS in air at a constant voltage of 0.6 V. The loss of cell performance over time is the same between all three sulfur species studied. The identity of sulfur species does not influence the rate of cathode deactivation. The drop in cell performance levels off as exposure time increases and the surface becomes saturated when 45% of the surface Pt atoms have adsorbed sulfur. The incomplete coverage of the Pt surface with sulfur suggests that it is strongly influenced by the presence of adsorbed oxygen on a working cathode. Cyclic voltammetry is a successful means of removing sulfur from the surface and restoring 92% of cell activity. The use of successive polarization curves on a sulfur poisoned catalyst is also an effective way of removing a large fraction of the adsorbed sulfur species and leads to 85% recovery of the cell activity.

Acknowledgements

The authors would like to thank the Office of Naval Research for support of this work. BDG is an American Society of Engineering Education postdoctoral fellowship.

References

[1] X. Cheng, Z. Shi, N. Glass, L. Zhang, J.J. Zhang, D.T. Song, Z.S. Liu, H.J. Wang, J. Shen, J. Power Sources 165 (2007) 739.
[2] R.J. Farrauto, C.H. Bartholomew, Fundamentals of Industrial Catalytic Processes, Blackie Academic and Professional, London, 1997, p. 267.
[3] E.B. Maxted, Adv. Catal. 3 (1951) 129.
[4] R. Mohtadi, W.K. Lee, S. Cowan, J.W. Van Zee, M. Murthy, Electrochem. Solid State Lett. 6 (2003) A272.
[5] R. Mohtadi, W.K. Lee, J.W. Van Zee, J. Power Sources 216 (2004) 138.
[6] R. Mohtadi, W.K. Lee, J.W. Van Zee, Appl. Catal. B: Environ. 56 (2005) 37.
[7] J.M. Moore, P.L. Adcock, J.B. Lakeman, G.O. Mepsted, J. Power Sources 85 (2000) 254.
[8] T. Rockward, I.G. Urdampilleta, F.A. Uribe, E.L. Brosha, B.S. Pivovar, F.H. Garzon, ECS Trans. 11 (2007) 821.
[9] I.G. Urdampilleta, F.A. Uribe, T. Rockward, E.L. Brosha, B.S. Pivovar, F.H. Garzon, ECS Trans. 11 (2007) 831.
[10] D.T. Chin, P.D. Howard, J. Electrochem. Soc. 133 (1986) 2447.
[11] Y. Nagahara, S. Sugawara, K. Shinohara, J. Power Sources 182 (2008) 422.
[12] H.A. Gasteiger, S.S. Kocha, B. Sompalli, F.T. Wagner, Appl. Catal. B: Environ. 56 (2005) 9.
[13] O.A. Baturina, K.E. Swider-Lyons, Proceedings of Power Sources, PA, Philadelphia, 2008, p. 185.
[14] T. Loucka, J. Electroanal. Chem. 31 (1971) 319.
[15] R.M. Spotnitz, J.A. Colucci, S.H. Langer, Electrochim. Acta 28 (1983) 1053.
[16] A.Q. Contractor, H. Lal, J. Electroanal. Chem. 93 (1978) 99.
[17] E.E. Swider, D.R. Rolison, Langmuir 15 (1999) 3302.
[18] K.E. Swider, D.R. Rolison, J. Electrochem. Soc. 143 (1996) 813.
[19] P. Marcus, E. Protopopoff, Surf. Sci. 161 (1985) 533.
[20] M.J. Foral, S.H. Langer, J. Electroanal. Chem. 246 (1988) 193.
[21] M. Szklarczyk, A. Czerwinski, J. Sobkowski, J. Electroanal. Chem. 132 (1982) 263.
[22] A.Q. Contractor, H. Lal, J. Electroanal. Chem. 96 (1979) 175.
[23] A.Q. Contractor, H. Lal, J. Electroanal. Chem. 103 (1979) 103.
[24] P.N. Ross, J. Electrochem. Soc. 126 (1979) 78.
[25] P.N. Ross, J. Electrochem. Soc. 126 (1979) 67.
[26] C. Quijada, J.L. Vazquez, J.M. Perez, A. Aldaz, J. Electroanal. Chem. 372 (1994) 243.
[27] X. Lin, W.F. Schneider, B.L. Trout, J. Phys. Chem. B 108 (2004) 250.
[28] Y. Garsany, O.A. Baturina, K.E. Swider-Lyons, J. Electrochem. Soc. 154 (2007) B670.
[29] W.Y. Shi, B.L. Yi, M. Hou, F.N. Jing, P.W. Ming, J. Power Sources 165 (2007) 814.
[30] Y.M. Sun, D. Sloan, D.J. Alberas, M. Kovar, Z.J. Sun, J.M. White, Surf. Sci. 319 (1994) 34.

[31] X. Lin, K.C. Hass, W.F. Schneider, B.L. Trout, J. Phys. Chem. B 106 (2002) 12575.
[32] X. Lin, W.F. Schneider, B.L. Trout, J. Phys. Chem. B 108 (2004) 13329.
[33] E. Najdeker, E. Bishop, J. Electroanal. Chem. 41 (1973) 79.
[34] G. Horanyi, E.M. Rizmayer, J. Electroanal. Chem. 206 (1986) 297.
[35] E. Lamypitara, Y. Tainon, B. Beden, J. Barbier, J. Electroanal. Chem. 279 (1990) 291.
[36] T. Loucka, J. Electroanal. Chem. 36 (1972) 355.
[37] T. Loucka, J. Electroanal. Chem. 36 (1972) 369.
[38] M.V. Mathieu, M. Primet, Appl. Catal. 9 (1984) 361.
[39] C. Quijada, A. Rodes, J.L. Vazquez, J.M. Perez, A. Aldaz, J. Electroanal. Chem. 398 (1995) 105.
[40] C. Quijada, A. Rodes, J.L. Vazquez, J.M. Perez, A. Aldaz, J. Electroanal. Chem. 394 (1995) 217.
[41] N. Ramasubramanian, J. Electroanal. Chem. 64 (1975) 21.
[42] E.S. Argano, S.S. Randhava, A. Rehmat, Trans. Faraday Soc. 65 (1969) 552.
[43] K. Sendt, B.S. Haynes, J. Phys. Chem. A 109 (2005) 8180.
[44] B. Nekrasov, Textbook of General Chemistry, Mir, Moscow, 1965, p. 300.
[45] R.E. Treybal, Mass-transfer Operations, McGraw-Hill, New York, 1980, p. 31.
[46] K. Baron, Thin Solid Films 55 (1978) 449.
[47] Z. Shi, D. Song, J. Zhang, Z.S. Liu, S. Knights, R. Vohra, N. Jia, D. Harvey, J. Electrochem. Soc. 154 (2007) B609.
[48] R.J. Koestner, M. Salmeron, E.B. Kollin, J.L. Gland, Surf. Sci. 172 (1986) 668.